Sensors and Actuators B 232 (2016) 571–576

Contents lists available at ScienceDirect

Sensors and Actuators B: Chemical

journal homepage: www.elsevier.com/locate/snb

Protein-based Y-junction optical micro-splitters with environment-stimulus-actuated adjustments

Si-Ming Sun[a], Yun-Lu Sun[a,**], Bo-Yuan Zheng[a], Pan Wang[b], Zhi-Shan Hou[c], Wen-Fei Dong[a], Lei Zhang[b], Qi-Dai Chen[a], Li-Min Tong[b], Hong-Bo Sun[a,c,*]

[a] State Key Laboratory on Integrated Optoelectronics, College of Electronic Science and Engineering, Jilin University, 2699 Qianjin Street, Changchun 130012, China
[b] Department of Optical Engineering, Zhejiang University, 38 Zheda Road, Hangzhou 310027, China
[c] College of Physics, Jilin University, 119 Jiefang Road, Changchun 130023, China

ARTICLE INFO

Article history:
Received 30 September 2015
Received in revised form 30 March 2016
Accepted 31 March 2016
Available online 1 April 2016

Keywords:
Femtosecond laser micro/nano-fabrication
Protein hydrogel
Micro/nano-waveguides
Y-junction optical splitters
Environment-stimulus-actuated adjustment

ABSTRACT

Herein, by using maskless and noncontact femtosecond laser direct writing (FsLDW) form protein aqueous ink, protein-based Y-junction optical micro/nano-splitters (PYOMs) have been readily customized with environmental-stimulus-actuated light-splitting adjustments for the first time to our knowledge. Bio/eco-compatible protein-based biopolymer successfully acted as the ideal alternative of artificial polymers for optical waveguide devices. Based on flexibly programmable "one-step" FsLDW, applicable shape-symmetric PYOMs were facilely fabricated with tailorable light-power-splitting ratios (from ~1:1 to ~3:1 in air). Significantly, via environmental responses and sensitivity of protein hydrogels, another type of "heterogeneous" PYOMs exhibited "smart" dynamic adjustments of light-power-splitting ratios by simply tuning surrounding chemical stimuli for example of pH value (~1:1 in air, ~1.35:1 in pure water, and 1.48:1–1.85:1 under pH 2.0–6.0), showing their application promise for optical sensing and environment-signal-actuated tunable micro/nano-optics.

1. Introduction

Recently, such distinctive and even irreplaceable multi-merits (e.g., good eco/bio-compatibility [1–3], degradability and implantable ability [2], diverse functionalities [1–5], and facile modification [1–5]) do the protein-derived biopolymers have, that various photonic and optical cutting-edge applications are realized with proteins. They not only overcome limitations of synthetic polymers on eco/bio-compatibility and multi-functionalization, but also open great opportunities for novel optical/photonic bio-engineering and biosystems with various functions [1,2,4–8]. Especially, the convenient functionalization with detecting probes [1,7], inherent bio-recognition (e.g., antibody proteins and avidin) [8], and environmental sensitivities (e.g., pH or ionic strength responsive swelling and shrinking) of protein hydrogels [2–5] can enable various sensing or environment-signal-actuated devices. So far, protein-based biopolymers and hydrogels have been increasingly utilized to obtain miniaturized optical waveguide devices for fields like eco/bio-compatible optical micro/nano-waveguides [6,7], biosensing [8], and flexible biophotonics [6]. However, in previous works, protein-based biopolymers were more often used to fabricate single-waveguide optical micro/nano-devices with relatively simple geometries and less structure details. More importantly, the functionalities (particularly novel sensing or actuating functions) were obviously limited by the inflexible and less-detailed device design and micro/nano-fabrication [6–8]. For instance, Y-junction-based optical micro-splitters/couplers, a fundamental and key integrated photonic device [9,10], were not reported using protein-derived biopolymers as far as we know. Whereas micro/nano-waveguide devices (including Y-junction-based optical micro-splitters/couplers) are more needed in many situations for not only traditional integrated photonics [9,10], but also novel utilizations including lab-on-a-chip integrated sensors [11–13], ultrasensitive Young interferometer biodetection [14], and spatial monitoring in microfluidics [15,16]. The absence of complex-shaped protein-based waveguide micro/nano-devices (e.g., Y-junction elements) might limit the proportion of biomaterials used, high-level integration, multiplexing, and var-

* Corresponding author at: State Key Laboratory on Integrated Optoelectronics, College of Electronic Science and Engineering, Jilin University, 2699 Qianjin Street, Changchun 130012, China.
** Corresponding author.
E-mail addresses: sunyunlu@jlu.edu.cn (Y.-L. Sun), hbsun@jlu.edu.cn (H.-B. Sun).

http://dx.doi.org/10.1016/j.snb.2016.03.164
0925-4005/

ious functionalizations of the emerging protein-based photonic micro/nano-biosystems, especially, for new-type sensing, tuning and actuation [2,4].

Herein, commercial bovine serum albumin (BSA) biomacromolecules acted well as "green prepolymers" to build novel protein-hydrogel-based Y-junction optical micro/nano-splitters (PYOMs) with distinct features (e.g., facile and flexible customization of light-splitting ratio, environment-stimulus-actuated light-splitting tuning). The promising femtosecond laser direct writing (FsLDW) approach was applied to readily realize noncontact and maskless fabrication of PYOMs from BSA aqueous ink [2,4,5,8]. As a kind of Fs-laser-aided three-dimensional (3D) printing approach, versatile FsLDW owns 3D nano-resolution and high controllability [17–19,20]. So excellent morphology quality (~5-nm average roughness, Ra, [2]) was ensured along with arbitrarily designed device-geometries of PYOMs, and consequently, applicable prototyping performances of light guiding and splitting were successfully achieved. Significantly, a "semi-transparent mirror" could be facilely integrated at the fork region of a PYOM via localized crosslinking-degree "heterogenization" during programmable one-step FsLDW. Hence, the light-intensity splitting ratios in air of shape-symmetric PYOMs could be readily tailored. More interestingly, another "heterogeneous" PYOM was ingeniously designed and delicately FsLDW-customized to have light-power-splitting ratios with environment-actuated "smart" adjustment, namely, pH-responsive tuning capability, which could also be used for sensing applications and has not been reported so far to our knowledge [10,21,22].

2. Experiments

During FsLDW, two-photon-absorption crosslinking of BSA biomacromolecules occurred under irradiation of the focused laser beam (Fs-laser: 800-nm central wavelength, 80-MHz repetition rate, 120-fs pulse width. Oil-immersed objective lens (OL): 60×; numerical aperture, 1.35) with the help of photosensitizer methylene blue (MB) [2]. By computer-controlled 3D scanning of the laser focal spot, freely designed PYOMs were FsLDW-customized facilely on MgF_2 slices from BSA aqueous ink (BSA, 500 mg/mL; MB, 0.6 mg/mL) after water-rinsing development. The refractive index (RI) of MgF_2 substrate (1.39) is lower than that of FsLDW-prepared protein micro/nano-hydrogels (~1.55 in air and ~1.45 in water [2,4]). So, all the PYOMs in this work were fabricated on MgF_2 substrates to cause total reflection and light propagation along protein-based waveguide devices [8,9]. Optimal FsLDW-processing parameters were applied in comprehensive consideration of fabrication quality and elapsed time (laser power measured before OL, ~20 mW; scanning step, 100 nm; exposure time on single point, 1000 μs). Furthe more, the self-built FsLDW system was equipped with an output feedback system and proper enclosure in the lab (local temperature, 22+/−0.2 °C; relative humidity, ~20%). As a result, the FsLDW system was maintained stable enough to guarantee high reproducibility and "self-smoothing"-induced excellent morphology of PYOMs (average roughness (Ra), as low as ~5 nm) [2].

3. Results and discussion

As shown in Fig. 1, fine PYOMs displayed various device-geometries for prototyping demonstration via characterizations with scanning electron microscopy (SEM) and atomic force microscopy (AFM). In Fig. 1, branch number, 1 × 2 or 1 × 4; line widths, ~500 nm (samples 3 of Fig. 1(a)–(c)), ~1 μm (samples 1 and 2 of Fig. 1(a) and (b)), and ~2 μm (samples 1 and 2 of Fig. 1(c)); samples 1, ~57.1° opening angles, 30-μm radius of curvature of arc parts; samples 2 and 3, ~33.6° opening angles, 50-μm radius of curvature. Thus, as the premises of the practical applications (light guiding and splitting), two factors were well implemented including highly designable device-geometries and reproducible high-quality morphology of FsLDW-fabricated PYOMs.

Satisfactory prototyping performances of light guiding and splitting could be successfully obtained as proved by optical microscopy (OM) images in Fig. 2. According to our previous work [8], as-formed protein-based waveguide micro/nano-devices have transmission windows of around ~530 nm and ~680 nm. At the present stage, we use both green and red light just for function demonstration and prototyping tests, which is more convenient for operation and observation. For further detailed improvements, more common near-infrared or infrared light can be mainly used to reduce photo-thermal effects and to facilitate practical applications of these protein-based optical waveguide micro/nano-devices. Here, 532-nm light from a semiconductor laser was used for visually demonstrating optical performances of 1 × 4 PYOMs with 2-μm line width [Fig. 2(a)]. Considering the convenient and flexible integration of fine functional secondary structures in Y crotches during one-step FsLDW, micro-scale waveguide width (2 μm here) was adopted for prototype demonstration. With a silica fiber nano-taper, 532-nm incident light was launched into the PYOMs by evanescent field coupling [8,9]. And the emergent light at the output ends could be captured and analyzed with a CCD camera or a spectrum detector [Fig. 2(b)]. Output light from ends of PYOMs was showed in dark-field OM images of Fig. 2(c). Fig. 2c-1 corresponds to the PYOM in Fig. 2a-1 and b-1 (~57.1° opening angles and 30-μm radius of curvature of arc parts); Fig. 2c-2 is for the PYOM in Fig. 2a-2 and b-2 (~33.6° opening angles and 50-μm radius of curvature). Obviously, light loss of the PYOM in Fig. 2a-2 and b-2 was smaller than that of the PYOM in Fig. 2a-1 and b-1. It might be caused by lower transmission loss at arc parts and splitting loss at Y-parts, respectively owing to smaller radian and opening angle. Although coupling efficiency might be relatively low because of easy evanescent field coupling method, applicable light guiding and splitting were proved experimentally for prototyping PYOMs on MgF_2 substrates [8,9]. Actually, as an approach to fabricate and position devices in one step [23], protein devices can be directly FsLDW-fabricated onto fixed fiber nano-tapers in a conformal way for improving the coupling efficiency.

Importantly, as designed in Fig. 3(a), the contraption of micro/nano-scale structure details of Y-branch parts could be satisfactorily implemented for tailoring light-power-splitting ratios of PYOMs. For a "homogeneous" shape-symmetric PYOM (Fig. 3a-1, b-1, c-1), FsLDW parameters for the whole device were 100-nm scanning step, ~20-mW laser power measured before OL, and 1000-μs exposure time on single point. For a "heterogeneous" but shape-symmetric PYOM in Fig. 3a-2, b-2, c-2, the input microwaveguide and one branch (cyan part in Fig. 3a-2, up branch in Fig. 3b-2, c-2) were FsLDW-fabricated as a whole "S"-style microwaveguide with 100-nm scanning step. And 70-nm scanning step was used for the other branch (red part in Fig. 3a-2, below branch in Fig. 3b-2, c-2). Meanwhile, other FsLDW parameters kept the same as those applied above. Then, PYOMs were obtained fully as designed and shown in Fig. 3(b) (device geometry: branch number, 1 × 2; line width, ~2 μm; opening angle, ~33.6°; radius of curvature, 50 μm). According to previous work [2–4], smaller FsLDW scanning step should result in higher protein crosslinking degree and then higher RI of FsLDW-fabricated protein hydrogel. Thus, localized "heterogenization" of protein crosslinking degree and RI were achieved for the PYOM in Fig. 3b-2 and c-2 during high-controllable one-step FsLDW with nano-resolution [3]. In consequence, an "interface" structure was obliquely placed and readily integrated in the Y-branch part [Fig. 3b-2]. It functioned like a "half-transparent/half-reflecting mirror" to tailor the light-

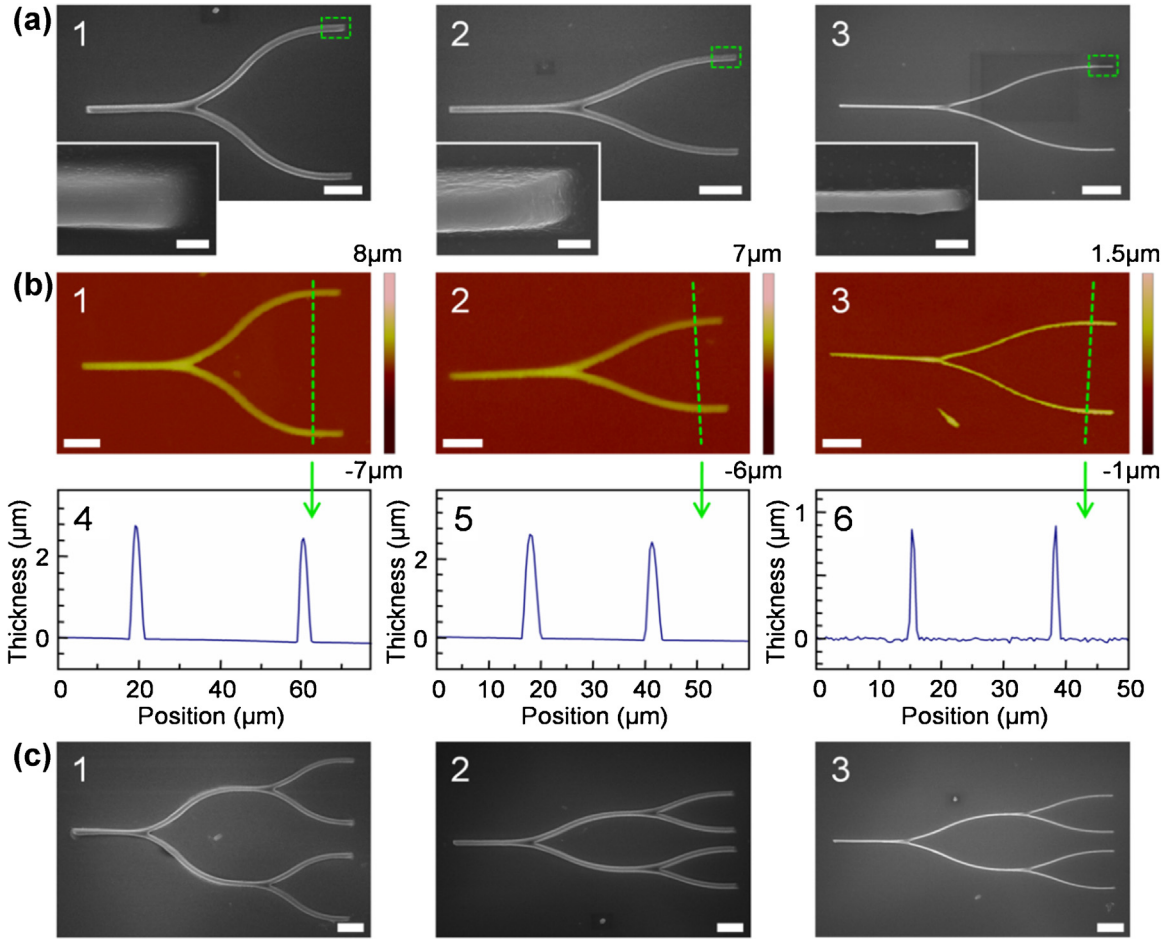

Fig 1. (a) SEM images of 1 × 2 PYOMs; scale bars, 10 μm. Insets, enlarged-view SEM images; scale bars, 1 μm. (b) 1–3, AFM graphs of 1 × 2 PYOMs in (a); scale bars, 10 μm. 4–6, Cross-section profiles corresponding to 1–3. (c) SEM images of 1 × 4 PYOMs; scale bars, 10 μm.

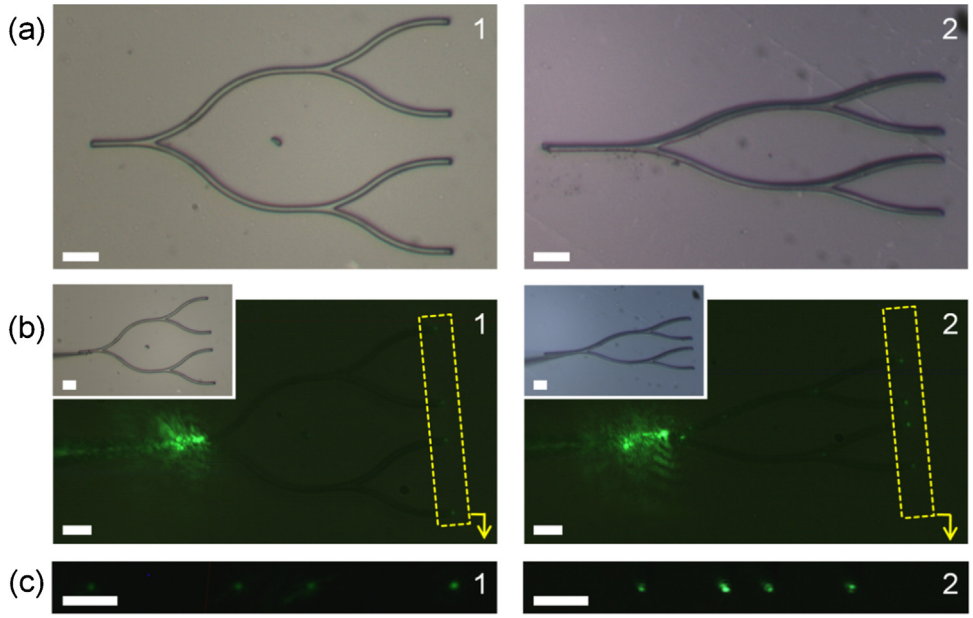

Fig. 2. (a) OM images of 1 × 4 PYOMs; scale bars, 10 μm. (b) Dark-field OM images of 1 × 4 PYOMs in (a) coupled with 532-nm light; scale bars, 10 μm. Insets, corresponding OM images of 1 × 4 PYOMs coupled with silica fiber nano-tapers; scale bars, 10 μm. (c) Dark-field OM images of output ends of 1 × 4 PYOMs in (b); scale bars, 10 μm.

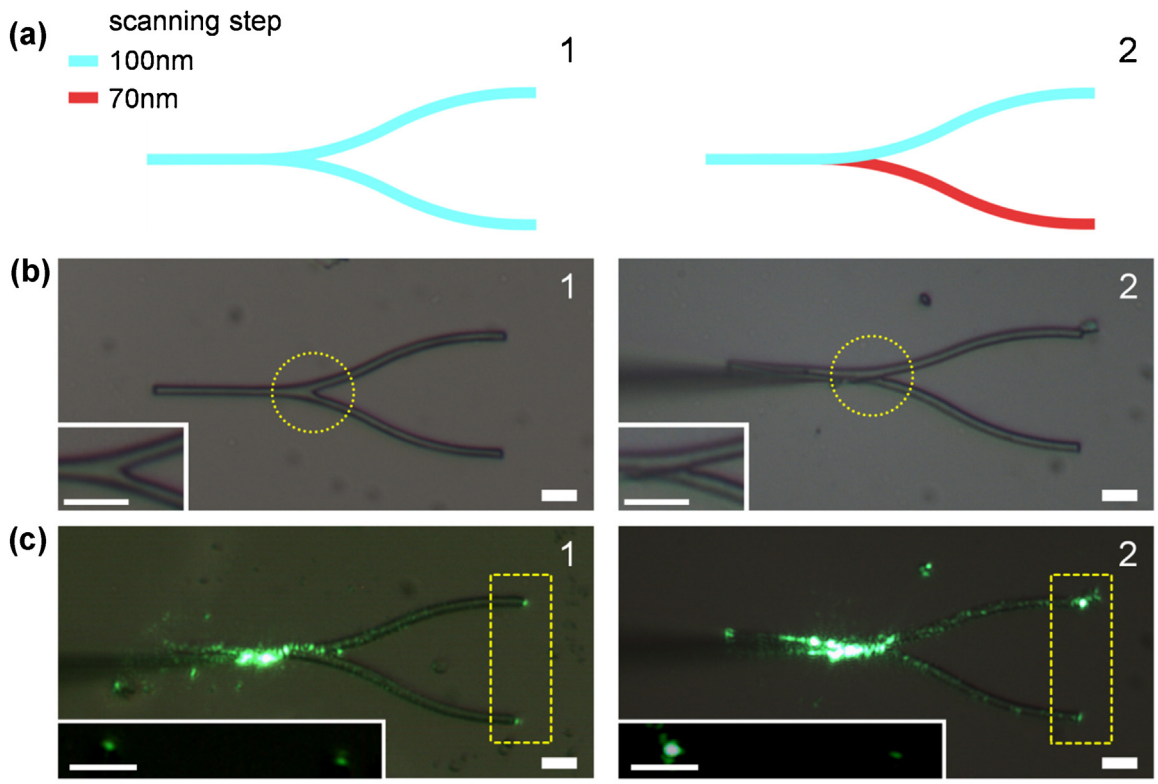

Fig. 3. (a) Schematic diagrams of 1 × 2 "homogeneous" (1) and "heterogeneous" (2) PYOMs. (b) OM images of 1 × 2 "homogeneous" (1) and "heterogeneous" (2) PYOMs; scale bars, 10 μm. Insets, enlarged-view OM images of Y-branch parts; scale bars, 10 μm. (c) OM images of 1 × 2 "homogeneous" (1) and "heterogeneous" (2) PYOMs in (b) coupled with 532-nm light; scale bars, 10 μm. Insets, enlarged-view dark-field OM images of output ends of 1 × 2 PYOMs; scale bars, 10 μm. (For interpretation of the references to color in the text, the reader is referred to the web version of this article.)

power-splitting ratio. Further, the light-power-splitting ratio might be changed flexibly as needed by adjusting placing angle, integrated position, and RI difference of the "mirror"-like "interface" structure. In addition, the local gray values of output light in dark-field-OM images were accumulated as the index of output intensity for estimating light-intensity-splitting ratios [8,9]. So, in Fig. 3(c), the light-intensity-splitting ratios in air of shape-symmetric PYOMs could be facilely customized from ~1:1 ("homogeneous" PYOMs) to ~3:1 ("heterogeneous" PYOMs) or larger via nano-resolution and high-controllable one-step FsLDW.

Furthermore, another type of "heterogeneous" PYOMs were designed with the same device geometry as that of Fig. 3a-1, but different exquisite collocation of protein FsLDW-crosslinking degree [see Fig. 4(a)]. In Fig. 4(a), the protein-FsLDW scanning steps were 70 nm for the red branch, and 100 nm for the input waveguide (cyan) and the other branch (blue). Noticeably, the connecting interfaces between the input waveguide (cyan part) and braches (red and blue parts) of the PYOM were symmetrically positioned vertically to the light-propagating direction. So, as prototyping demonstration in Fig. 4b-1, c, and d for this design, the 532-nm input light was symmetrically split (~1:1 light-power-splitting ratio) by the PYOM in air without asymmetrically swelling. More significantly, the as-designed PYOM was endowed with ingenious environment-responsive "smart"-tuning capacity of the light-intensity-splitting ratio in aqueous environments. Owing to the instinct features proved previously [2–4], FsLDW-formed protein-based micro/nano-hydrogels could equilibrium swell to different extents corresponding to varying surrounding signals, for example, pH values. For this equilibrium swelling, the geometries (mainly the line width) and especially the RIs of the PYOM might be stimulated to change during pH variation [2,4] [see Fig. 4(b)]. Consequently, the light-power-splitting ratio could be tuned dynamically and environment-responsively (so-called "smart") as shown in Fig. 4(d) (~1:1 in air, ~1.35:1 in pure water, and ~1.48:1 to ~1.85:1 under pH 2.0–6.0).

In Fig. 5(a) and (b), indicated by Rsoft simulations (Beam propagation method) for a "homogeneous" PYOM as designed in Fig. 3a-1, more light might be leaked out from junction and especially blending parts of the equilibrium-swollen PYOM in pure water than that in air (Fig. 5(a) in air: protein hydrogel RI, 1.55, surrounding RI, 1.0; Fig. 5(b) in pure water: protein hydrogel RI, 1.45, surrounding RI, 1.33) [2,4]. The reason might be that equilibrium swelling decreased RI of protein hydrogel and then the difference of RIs of the PYOM and surroundings as observed in our previous work [2,4]. So, for more obviously exhibiting environment-stimulus-actuated light-splitting adjustments, we designed PYOM devices here with ~33.6° opening angle (relatively large for optical splitters) and 50-μm waveguide radius of curvature (relatively small for light propagation) for properly obvious and tunable light leak. Similar mechanisms probably functioned during pH-tuning processes in Fig. 4(c) and (d). Less densely crosslinked branch 2 (blue branch in Fig. 4(a) and lower branch in Fig. 4(b) and (c)) swelled more obviously at first when operation environments changed from air to pure water (pH 7.0) and then to pH 6.0. More decreased RI of branch 2 resulted into higher light loss than branch 1. While the equilibrium swelling of branch 2 approached to limitation with slowdown changes along with further pH decrease (6.0–2.0), the other branch (branch 1 in Fig. 4(c)) with higher crosslinking density swelled to extent comparative with branch 2. So, the light-power-splitting ratio started to fall back from ~1.85:1 (pH 6.0) to ~1.48:1 (pH 2.0). Compared with other tunable Y-junction-based optical power microsplitters (e.g., fiber-couple-length tuning [22], "Mach-Zehnder" method [22], micro-electro-mechanics [21], acousto/electro/thermo-optic

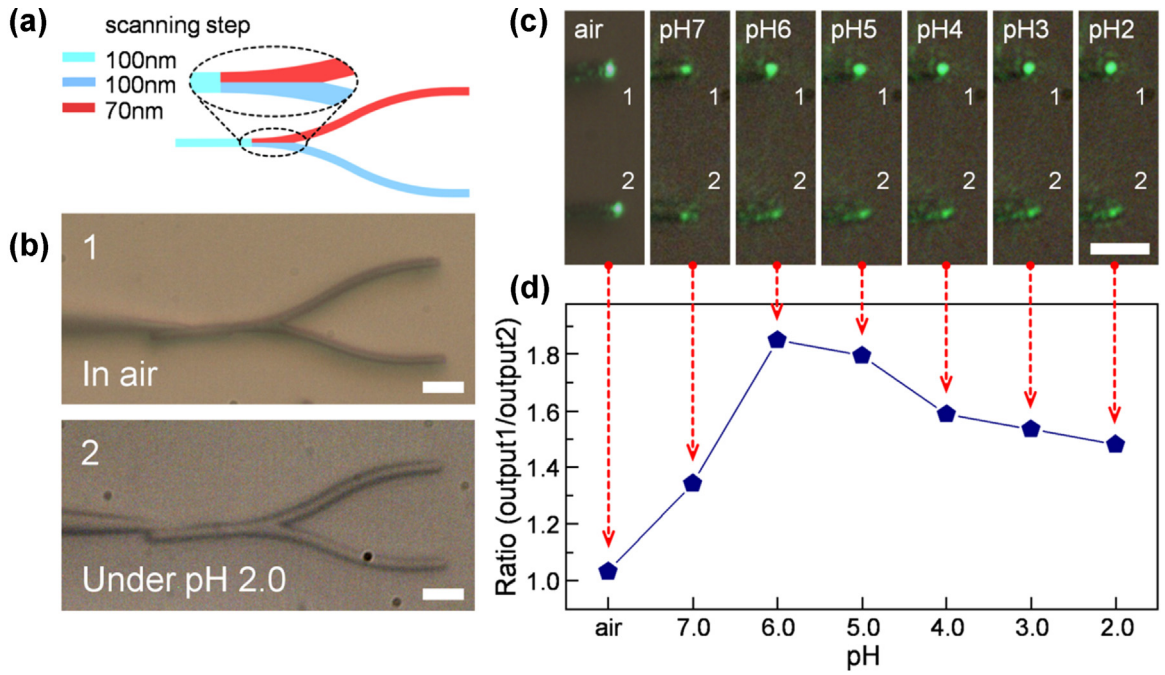

Fig. 4. (a) Schematic diagram of another tpye of the 1 × 2 "heterogeneous" PYOM. (b) OM images of the 1 × 2 the PYOM in air (1) and under pH 2.0 (2); scale bars, 10 μm. (c) OM images of output light from the 1 × 2 the PYOM in (b) coupled with 532-nm light in different environments; scale bars, 10 μm. (d) Light-intensity-splitting ratios (output1/output2) of the PYOM in (b) in different environments. (For interpretation of the references to color in the text, the reader is referred to the web version of this article.)

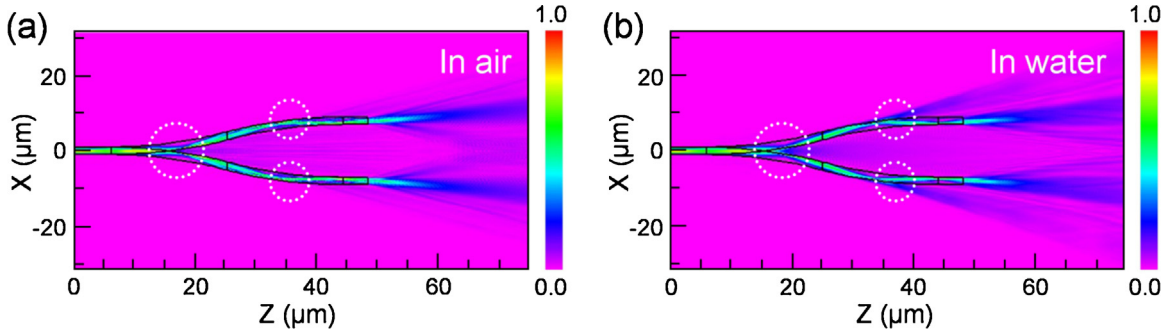

Fig. 5. (a) Rsoft simulation of a "homogeneous" PYOM in air with 532-nm incident light. (b) Rsoft simulation of a "homogeneous" PYOM equilibrium swollen in water with 532-nm incident light.

deflections [22]), this bio/eco-compatible PYOM possesses brand-new-style chemical-stimulus-responsive "smart" tuning, and fine "configurability" via easy fabrication and structural alteration.

Additionally, we tested the relevant properties of the protein gel under different temperatures, especially the optical properties like the refractive index of the protein gel (see the Supplementary information Fig. S1). The refractive index of the protein gel gets lower when the temperature increases, which is quite similar to some artificial polymers (e.g., polymethyl methacrylate, PMMA) as reported in others' work [24–26]. But here, we applied relatively low-energy input light, and operated our protein devices in aqueous environments in many cases which should be helpful for heat dissipation. So, the light propagating in the protein waveguides may not produce temperature increase large enough for obviously changing devices' performances. Meanwhile, as proved in our previous work, chemical surrounding signals like pH value should induce much larger change of protein devices than that caused by possible temperature variation (let alone that there may be no obvious temperature changes) [2,4,5]. In a word, the photo-thermal influence on the properties of protein gel and optical devices is so minor (especially compared with chemical signals) that it may be ignored in this work at the present stage. On the other hand, the red and infrared light with probable lower absorption also applies to these protein-based optical waveguide micro/nano-devices [8], which may help for reducing any possible photo-thermal effects in our work.

4. Conclusions

In summary, a distinct FsLDW-based route was demonstrated to achieve novel prototyping PYOMs. Good bio/eco-biocompatibility might be realized with proteins (BSA) as natural-product bio-alternatives of artificial polymers. The arbitrary FsLDW fabrication and nano-resolution hyperfine structures were valuable for adaptability and diversity of practical applications. Then, owing to high-quality device geometries and surface morphology, applicable optical performances (light propagating and splitting) were guaranteed for the PYOMs. More interestingly and significantly, highly tailorable (~1:1 to ~3:1) and further "smart" dynamically tunable light-power splitting (~1:1 in air, ~1.35:1 in pure water, and

about 1.85:1–1.48:1 under pH 6.0–2.0) were successfully implemented respectively for specially designed PYOMs via contraptions simply based on flexible manipulations of crosslinking density of protein micro/nano-hydrogels. By comprehensively combining above-mentioned features, PYOMs in this work hold great promise for frontier areas such as optical sensing, integrated optofluidics and biophotonics, and novel tunable micro/nano-photonics actuated by environmental signals.

Acknowledgments

This work was supported by the National Natural Science Foundation of China (NSFC) and the National Basic Research Program of China (973 Program) under grants #61590930, #2014CB921302, #91423102, #61435005 and #61378053.

Appendix A. Supplementary data

Supplementary data associated with this article can be found, in the online version, at http://dx.doi.org/10.1016/j.snb.2016.03.164.

References

[1] H. Tao, J.M. Kainerstorfer, S.M. Siebert, E.M. Pritchard, A. Sassaroli, B.J.B. Panilaitis, M.A. Brenckle, J.J. Amsden, J. Levitt, S. Fantini, D.L. Kaplan, F.G. Omenetto, Implantable, multifunctional, bioresorbable optics, Proc. Natl. Acad. Sci. U. S. A. 109 (2012) 19584–19589.
[2] Y.L. Sun, W.F. Dong, R.Z. Yang, X. Meng, L. Zhang, Q.D. Chen, H.B. Sun, Dynamically tunable protein microlenses, Angew. Chem. Int. Ed. 51 (2012) 1558–1562.
[3] B. Kaehr, J.B. Shear, Multiphoton fabrication of chemically responsive protein hydrogels for microactuation, Proc. Natl. Acad. Sci. U. S. A. 105 (2008) 8850–8854.
[4] Y.L. Sun, D.X. Liu, W.F. Dong, Q.D. Chen, H.B. Sun, Tunable protein harmonic diffractive micro-optical elements, Opt. Lett. 37 (2012) 2973–2975.
[5] Y.L. Sun, W.F. Dong, L.G. Niu, T. Jiang, D.X. Liu, L. Zhang, Y.S. Wang, Q.D. Chen, D.P. Kim, H.B. Sun, Protein-based soft micro-optics fabricated by femtosecond laser direct writing, Light: Sci. Appl. 3 (2014) e129, http://dx.doi.org/10.1038/lsa.2014.10.
[6] A.K. Manocchi, P. Domachuk, F.G. Omenetto, H. Yi, Facile fabrication of gelatin-based biopolymeric optical waveguides, Biotechnol. Bioeng. 103 (2009) 725–733.
[7] S.T. Parker, P. Domachuk, J. Amsden, J. Bressner, J.A. Lewis, D.L. Kaplan, F.G. Omenetto, Biocompatible silk printed optical waveguides, Adv. Mater. 21 (2009) 2411–2415.
[8] Y.L. Sun, S.M. Sun, P. Wang, W.F. Dong, L. Zhang, B.B. Xu, Q.D. Chen, L.M. Tong, H.B. Sun, Customization of protein single nanowires for optical biosensing, Small 11 (2015) 2869–2876.
[9] L.M. Tong, J.Y. Lou, R.R. Gattass, S.L. He, X.W. Chen, L. Liu, E. Mazur, Assembly of silica nanowires on silica aerogels for microphotonic devices, Nano Lett. 5 (2) (2005) 259–262.
[10] Y.O. Noh, H.J. Lee, Y.H. Won, M.C. Oh, Polymer waveguide thermo-optic switches with −70 dB optical crosstalk, Opt. Commun. 258 (2006) 18–22.
[11] G. Calafiore, A. Koshelev, S. Dhuey, A. Goltsov, P. Sasorov, S. Babin, V. Yankov, S. Cabrini, C. Peroz, Holographic planar lightwave circuit for on-chip spectroscopy, Light: Sci. Appl. 3 (2014) e203, http://dx.doi.org/10.1038/lsa.2014.84.
[12] P. Wang, Y.P. Wang, L.M. Tong, Functionalized polymer nanofibers: a versatile platform for manipulating light at the nanoscale, Light: Sci. Appl. 2 (2013) e102, http://dx.doi.org/10.1038/lsa.2013.58.
[13] M.C. Estevez, M. Alvarez, L.M. Lechuga, Integrated optical devices for lab-on-a-chip biosensing applications, Laser Photonics Rev. 6 (2012) 463–487.
[14] A. Ymeti, J. Greve, P.V. Lambeck, T. Wink, S.W.F.M. van Hovell, T.A.M. Beumer, R.R. Wijn, R.G. Heideman, V. Subramaniam, J.S. Kanger, Fast, ultrasensitive virus detection using a young interferometer sensor, Nano Lett. 7 (2007) 394–397.
[15] A. Llobera, J. Juvert, A. González-Fernández, B. Ibarlucea, E. Carregal-Romero, S. Büttgenbach, C. Fernández-Sánchez, Biofunctionalized all-polymer photonic lab on a chip with integrated solid-state light emitter, Light: Sci. Appl. 4 (2015) e271, http://dx.doi.org/10.1038/lsa.2015.44.
[16] F. Sapuppo, F. Schembri, L. Fortuna, A. Llobera, M. Bucolo, A polymeric micro-optical system for the spatial monitoring in two-phase microfluidics, Microfluid. Nanofluid. 12 (2012) 165–174.
[17] K. Sugioka, Y. Cheng, Ultrafast lasers-reliable tools for advanced materials processing, Light: Sci. Appl. 3 (2014) e149, http://dx.doi.org/10.1038/lsa.2014.30.
[18] W. Xiong, Y.S. Zhou, X.N. He, Y. Gao, M.M. Samani, L. Jiang, T. Baldacchini, Y.F. Lu, Simultaneous additive and subtractive three-dimensional nanofabrication using integrated two-photon polymerization and multiphoton ablation, Light: Sci. Appl. 1 (2013) e6, http://dx.doi.org/10.1038/lsa.2012.6.
[19] M. Schumann, T. Buckmann, N. Gruhler, M. Wegener, W. Pernice, Hybrid 2D-3D optical devices for integrated optics by direct laser writing, Light: Sci. Appl. 3 (2014) e175, http://dx.doi.org/10.1038/lsa.2014.56.
[20] D. Wu, J. Xu, L.G. Niu, S.Z. Wu, K. Midorikawa, K. Sugioka, In-channel integration of designable microoptical devices using flat scaffold-supported femtosecond-laser microfabrication for coupling-free optofluidic cell counting, Light: Sci. Appl. 4 (2015) e228, http://dx.doi.org/10.1038/lsa.2015.1.
[21] Q. Chen, W. Wu, G. Yan, Z. Wang, Y. Hao, Novel multifunctional device for optical power splitting, switching, and attenuating, IEEE Photonics Technol. Lett. 20 (2008) 632–634.
[22] S. Xiao, Q. Zeng, J. Wang, H. Zhao, H. Chi, Y. Wang, F. Liu, X. Zhu, Tunable optical splitter technology, Proc. SPIE 4870 (2002) 532–539.
[23] S. Juodkazis, V. Mizeikis, S. Matsuo, K. Ueno, H. Misawa, Three-dimensional micro-and nano-structuring of materials by tightly focused laser radiation, Bull. Chem. Soc. Jpn. 81 (2008) 411–448.
[24] T. Watanabe, N. Ooba, Y. Hida, M. Hikita, Influence of humidity on refractive index of polymers for optical waveguide and its temperature dependence, Appl. Phys. Lett. 73 (1998) 1533–1535.
[25] S. Juodkazis, N. Mukai, R. Wakaki, A. Yamaguchi, S. Matsuo, H. Misawa, Reversible phase transitions in polymer gels induced by radiation forces, Nature 408 (2000) 178–181.
[26] S. Juodkazis, V. Mizeikis, K.K. Seet, H. Misawa, Mechanical properties and tuning of three-dimensional polymeric photonic crystals, Appl. Phys. Lett. 91 (2007) 241904.

Biographies

Si-Ming Sun is pursuing his Ph.D. at Jilin University, China. His research interest has been focused on the technique of femtosecond laser direct writing to fabricate macro/nano devices.

Yun-Lu Sun received his Ph.D. in Physical Electronics from Jilin University, China, in 2015. He is currently an assistant professor at Jilin University. His research interests include laser micro/nano-fabrication, biophotonics and bioelectronics.

Bo-Yuan Zheng is currently a Master student at Jilin University, China. His research interest has been focused on the technique of femtosecond laser direct writing to fabricate macro/nano devices.

Pan Wang received his Ph.D. degree in Optics Engineering from Department of Optical Engineering, Zhejiang University, China in 2013. He is currently a research associate at King's College London, United Kingdom. His research interests include nanophotonics and plasmonics.

Zhi-Shan Hou is currently a Master student at Jilin University, China. His research interest has been focused on the technique of femtosecond laser direct writing to fabricate macro/nano devices.

Wen-Fei Dong received his Ph.D. degree in Potsdam University, Germany in 2004. He is currently a researcher at Suzhou institute of biomedical engineering and technology, Chinese academy of sciences. His research interest has been in the area of bio-probes and nano-scale photonic and electrical sensors.

Lei Zhang received his Ph.D. degree in Chemistry from Department of Chemistry, Zhejiang University, China in 2006. He is currently an assistant professor at Zhejiang University. His research interests include micro/nano-fiber sensors, optofluidics, and plasmonics.

Qi-Dai Chen received his Ph.D. in Physics from the Institute of Physics, Chinese Academy of Sciences, China, in 2004. He is currently a full professor at Jilin University, China. His research interests include laser microfabrication and ultrafast laser spectroscopy.

Li-Min Tong received his B.S. and M.Sc. degrees in Physics and Ph.D. degree in Materials Science and Engineering from Zhejiang University, China in 1991, 1994 and 1997. He is currently a professor at Zhejiang University. His research interest has been in the area of nanophotonics and fiber optics.

Hong-Bo Sun received his Ph.D. in Electronic Science and Engineering from Jilin University in 1996. He is currently a full professor at Jilin University. His research interests have been focused on laser nanofabrication and ultrafast spectroscopy. He has published over 200 scientific papers in the above fields.